Further Progress in the Electrostatic Nucleation of Water Vapor

Michael Reznikov, Matthew Salazar,
Physical Optics Corp.
phone: (1)310-320-3088
contact e-mail: mreznikov@poc.com

Martin Page, Melixa Rivera-Sustache
ERDEC-CERL
phone: (1)217-373-3477

***Abstract*— The global demand for drinkable water is very high because 1.2 billion people in this world do not have access to drinking water and 2.4 billion have no adequate sanitation. At other hand, the planet atmosphere holds an enormous amount of water. Existing state-of-the-art "atmospheric water generation" (AWG) systems mostly work by the cooling of entire air flow below the dew point that requires the significant amounts of energy per liter of water. As a result, the cost of this water is similar to those of imported bottled water in small single-use plastic containers. Therefore, there is an urgent need for any technology that generates usable water in an energy-efficient manner. It is known that the native dipole moment of water molecule results in the nucleation of liquid phase on carriers of electrical charge due to the suppressed evaporation. Nevertheless, the practical implementation of electrostatic water nucleation (EWN) is still in the stage of laboratory demonstrations. The present work summarizes the theoretical background of the phenomenon and past experimental data, presents further experimental results and new data from practical implementation of EWN, and analyses options for the further development.**

I. Introduction

Drawing water from air (a so called atmospheric water generation, AWG) is a generic technology that produces potable water from water vapor in the air by a process that is a kind of dehumidification: difference is only in the product fluid, dehumidified air or the condensed moisture. The basic approach is to cool the atmospheric air below its dew point temperature, i.e. extract the specific heat of humid air and then the latent heat in the water content, for the water condensation. In fact, this approach, if utilizing the day/night temperature difference, is known from ancient times as dew wells or dew ponds. There are two opportunities for electrostatics to decrease the energy consumption at water vapor condensation: (a) the minimizing of parasitic air cooling by the enhancing of water delivery to the cooling surface by the electric field; and (b) the rejection of latent heat to the air due to the decreased heat capacity of electrically charged droplet.

We have reported before [1,2] that the ionization of air allows for ~16 - 20% dehumidification due to the dielectrophoretic (DEP) nucleation of polar water molecules on ions. The air ionization approach has the inherent restraint due to the limited charge of ion, which serves as a nucleation center. This restricts the equilibrium size of liquid phase (micro-droplets) that in turn elevates the equilibrium vapor pressure, i.e. the residual vapor pressure in the air. However, if electrospray droplets are used as nucleation centers, they are initially charged to the Rayleigh limit when electrostatic forces do not exceed those of surface tension. Due to the stronger electric field, these charged droplets attract the vapor and thus the size of micro-droplets increases [3]. This explains why the electrospray water droplets are mostly charged to 80-85% of the Rayleigh limit: they immediately start to collect the vapor from the air. Because the created droplets are still electrically charged and thus affected by the electric field, the bonus advantage of the electrospray is the direct deposition of liquid phase onto the cooling wall that minimizes the energy consumption for the cooling of air. For example, recently we have demonstrated the 57% improvement of condensation rate for the condensation of steam [3]. Of course, the effect of electrospray varies from 50% (if there is very hot ambient temperature and insufficient power is handled by the cooling system) to nothing in the cold environment and with the powerful cooling system.

In short words, the electrostatic enhancement of condensation is based on the combination of three phenomena:

1) Dielectrophoretic (DEP) nucleation of the vapor on electrically charged centers;

2) Electrohydrodynamic (EHD) flow of the vapor due to the drag by electrically charged droplets; and

3) Temporal (until droplets are discharged) decrement of the heat capacity in electrically charged droplets due to increased entropy.

II. Brief Theoretical Background [1]

A. Effect of Corona Discharge

When a water molecule is placed in a gradient electric field of magnitude E, such a polar molecule experiences DEP force $F_{dp} = \rho_o \mathrm{grad} E$ directed to the side of the increased field E, i.e. toward the electrically charged center of nucleation. This produces a gradient of the vapor concentration and the steady state occurs when the DEP drift and the local diffusion flows are equal, which leads to the classic Maxwell distribution of the vapor concentration, i.e., $n(r_0) = n_\infty \exp(U(r_0)/kT)$, where k is Boltzmann's constant, T is the absolute temperature, and the potential energy of a molecule at distance r_0 from point charge q is $U(r_0)$. This potential energy can be calculated by the integration of the DEP force from distance r_0 to infinity as follows:

$$U = \rho_0 \int_{r_0}^{\infty} gradEdr = \rho_0 q / (4\pi\varepsilon_0 r_0^{\,2}) . \qquad (1)$$

If this additional potential energy is accounted for, the classic Kelvin-Thomson equation

for the saturated vapor pressure, p^{β} near the surface of a charged drop with radius R

$$p_C^{\beta} = p_{\infty} \exp[\frac{2\gamma v^l}{kTR} - \frac{q^2 v^l}{32\pi^2 kT\varepsilon_0 R^4}(\frac{1}{\varepsilon^{\beta}} - \frac{1}{\varepsilon^l})], \qquad (2)$$

where v^i is a volume per single molecule in liquid, and p_{∞} is the pressure of saturated water vapor above a flat surface at temperature T, is modified to

$$p_M^{\beta} = p_C^{\beta} \exp[-\frac{\rho_0 q}{4\pi kTR^2}]. \qquad (3)$$

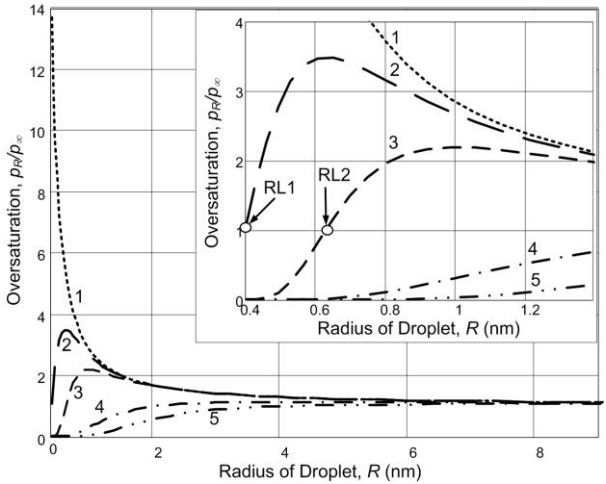

Fig. 1. Oversaturation of vapor pressure near the droplet of radius R, p_R, relative to the saturated vapor pressure over the flat surface of water, p_{∞}, that illustrates the effect of electric charge: 1 = neutral droplet; 2 and 3 = droplets with single and double electron charges, correspondingly, according to the classic Kelvin-Thomson equation (2); 4 and 5 = droplets with single and double electron charges respectively, according to the modified Kelvin-Thomson equation (3). Circles show the Rayleigh limits when droplet disintegrates due to electrical forces.

Thus the charged droplet acquires additional negative potential energy, which may be interpreted either as increased latent heat of evaporation or decreased effective surface tension in the basic Kelvin equation $p^{\beta} = p_{\infty} \exp(2\gamma v^l / kTR)$.

B. Effect of Electrospray

The dielectrophoretic potential of vapor molecules near the surface of charged droplet increases proportionally to the charge in the droplet and correspondingly adds to the latent heat for evaporation of this droplet. Fig. 2 illustrates that this increment in the evaporation energy is significant only for small, <10 μm, droplets, but the total latent heat for evaporation of these droplets is relatively small. As a result, the dielectrophoretic potential notably affects the stability of small droplets only.

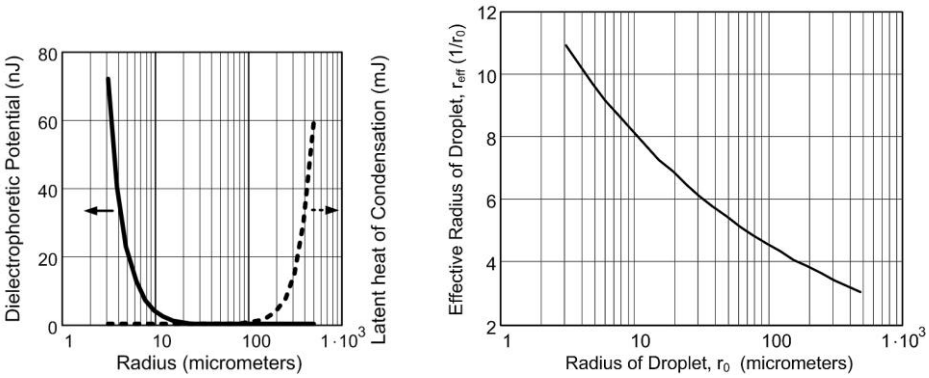

(a) (b)

Fig. 2. Effect of droplets charged to the Rayleigh limit: (a) - Dielectrophoretic potential of a droplet (solid line, left vertical axis) compared with the latent heat evaporation of this droplet (dotted line, right vertical axis). Note that the dielectrophoretic potential reaches a significant magnitude for a small, <10 μm, droplet, while the latent heat of condensation notably increases for larger droplets; (b) - Effective vapor collection radius, which is related to the distance where the dielectrophoretic force creates the centripetal flow of vapor. Note that the effective radius of vapor collection is presented relatively to the actual radius of droplet.

The effective radius for the collection of vapor is compared to the radius of a charged droplet in Fig. 2(b) where this effective radius as a distance where the dielectrophoretic potential exceeds the average energy of thermal fluctuations, kT , at temperature, T , where k is the Boltzmann constant. Thus the gradient of vapor pressure is created near the charged droplet and the real vapor pressure over the droplet surface depends on the vapor pressure in the surrounding space.

C. Thermodynamics of charged droplet.

Both equations (2) and (3) are related to the equilibrium of a water droplet of radius *R* with vapor. At this condition, the chemical potential of the molecule in the neutral droplet, $\mu^l(R,T)$, is equal to the chemical potential of a gas phase (vapor) water molecule near the surface of this droplet

$$\mu^{\beta}(R,T) = \mu^0(T) + kT\ln(p_{\infty}) + \frac{2\gamma v^l}{kTR}, \tag{4}$$

where $\mu^0(T)$ is the standard chemical potential of vapor, and p_∞ is the ambient vapor pressure. The modified Kelvin-Thomson equation is directly derived from

$$\mu^{\beta}(R,T,q) = \mu^{\beta}(R,T) - \Delta\mu_{DEP}, \tag{5}$$

where $\Delta\mu_{DEP} = \frac{q^2 v^l}{32\pi^2\varepsilon_0 R^4} + \frac{q\rho_0}{4\pi\varepsilon_0 R^2}$ is the decrement of chemical potential due to dielectrophoretic forces. We are neglecting here the impact of vapor polarization in the uniform field, $\Delta\rho_0(r) = \alpha E(r)$, due to the low polarizability of water molecules, α, and the relatively low electric field. The polarization of vapor as a dielectric shell (Born ener-

gy) $\Delta\mu_{pol}^{\beta} = q^2 \big/ 8\pi\varepsilon^{\beta}\varepsilon_0 R$ was also neglected because it is ~10^{-20} J for R = 10 nm and a single electron charge, $q = e = 1.6\cdot10^{-19}$ C, while the dielectrophoretic contribution to the chemical potential is ~ $0.9\cdot10^{-12}$ J under same conditions.

The outcome from Eq. (5) is that the heat capacitance of the charged droplet is decreased. Indeed, at a constant droplet volume of $4\pi R^3/3$, the heat capacitance is proportional to the second derivative of Gibbs energy, $G = N\cdot\mu^l$, where N is the number of molecules in the cluster (droplet), and the chemical potential in the liquid, μ^l, is defined by Eq. (5). Therefore, the isochoric heat capacitance of the droplet is defined as

$$C_{V,N} = -T\left(\frac{\partial^2 G}{\partial T^2}\right)_{V,N} = -T\cdot N\left(\frac{\partial^2(\mu_n - \Delta\mu_{DEP})}{\partial T^2}\right)_V, \qquad (6)$$

where μ_n is the chemical potential in the neutral droplet according to Eq. (4). Therefore, the electric charge should decrease the heat capacitance of the droplet. This speculative conclusion is supported by experimental data from [4] where the effect of electric charge on $C_{V,N}$ was investigated by the measuring the evaporation rate of charged clusters. On other hand, the enthalpy of the charged droplet is higher than that of the same number of molecules in bulk neutral water. The excess enthalpy is stored as energy of electric polarization. This is supported by numerical modeling and experimental data [5].

In the context of electrostatic enhancement of condensation, the decrement of heat capacitance of electrically charged droplet means that the temperature of droplet decreases at the discharge on the grounded condensing wall. In other words, electrostatic energy partially replaces the latent heat of condensation during the nucleation on the charged nuclei that reduces the thermal load on the heat pump (refrigerator).

III. Experiments

A. Experimental Setup of Condenser.

The experimental setup (see Fig. 3a) implements a thermoelectric cold plate cooler, CP-065 (TE Technology, Inc., Traverse City, MI), which provides cooling power up to 65 W while consuming up to 5.5 A of 24 VDC.

The evaluated system consists of two main stages — the moisture separator and the water condenser. The moisture separator, shown in Fig. 4(a), uses corona discharge, directed across the airflow. The microdroplets are created on ions and this concentrated moist air (actually fog) is supplied to the condenser shown in Fig. 3(b).

The core component of the electrically enhanced condenser is the array of electrospray heads shown in Fig. 4(b) and previously used for the steam condenser [3]. Each head contains the grounded electrostatic dripper tip, which supplies the liquid to electrospray needle (emitter) at the high voltage. The electrospray is stabilized by the grounded extraction ring in front of the needle. This results in the stable electrospray invariably on the distance to the condensing wall and humidity of the air.

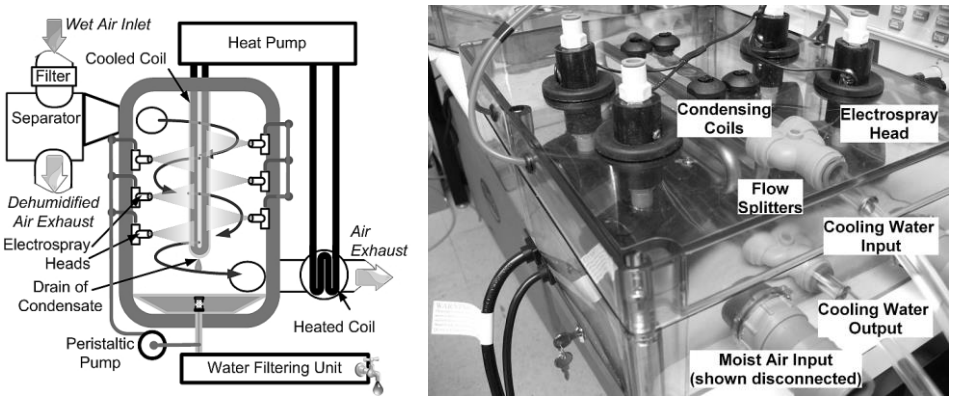

(a) (b)

Fig. 3. Experimental setup for evaluation of electrically enhanced harvesting of water vapor from the air: (a) Scheme of setup; (b) The close look of electrically enhanced condenser.

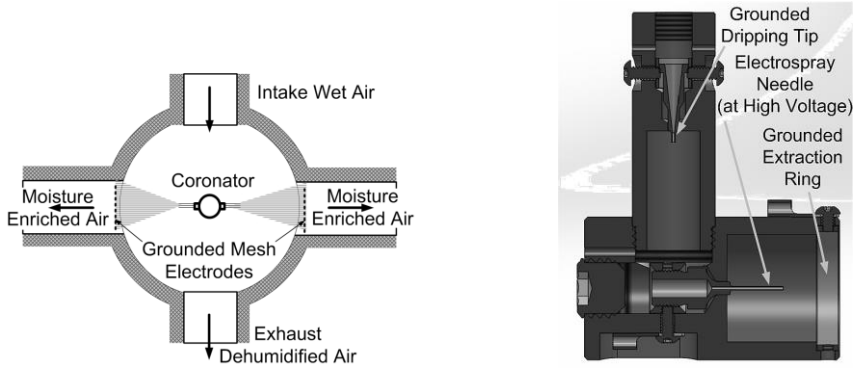

(a) (b)

Fig. 4. Schemes of main electrostatic components: (a) - moisture separator; (b) – electrospray emitter.

The electrospray across the airflow in the condenser works like a wiper for humidity — the moisture is collected and delivered to the cooled coil, which extracts the latent heat without the necessity to cool the airstream. The heat exchange with the condensed water is provided by the stainless steel heat exchangers, LC-SSX1 from the same vendor (TE Technology, Inc.) as the CP-065 heat pump.

B. Experimental Data for Condenser

The power supplied to the evaluated bench-scale prototype during the tests was monitored and kept stable during all tests. The prototype was tested at full cooling power (65 W) and at reduced cooling power (14 W) in the chiller. During the comparative series of tests, the prototype was ran in three regimes: (1) Full system (all components ON); (2) Electrospray OFF with corona separator and cooler ON; and (3) Both electrospray and corona separator OFF, cooling system ON. Results of these tests are presented in Fig. 5.

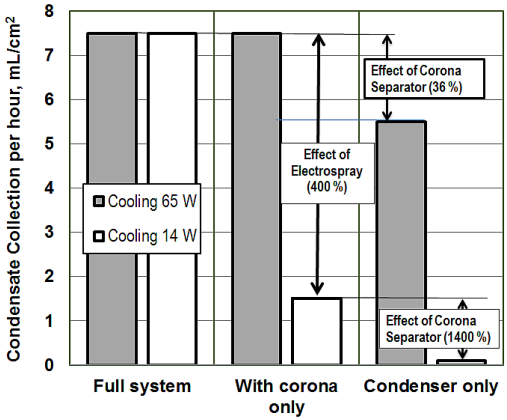

Fig. 5. Effect of corona vapor separator and electrospray on the condenser performance at varied cooling power (65 W and 14 W).

This comparative test clearly demonstrated that the electrospray dramatically, by 5 times, improves the water vapor harvesting rate if the cooling power is reduced to 14 W and correspondingly the temperature of condensing coil increased to 22°C. At the high cooling power (65 W), the moisture harvesting rate increased by 36% (from 5.5 mL/hr to 7.5 mL/hr) due to the corona separator while the effect of electrospray on the harvesting rate is negligible because the applied cooling power was excessive, which diminishes the effect of electrospray, as we demonstrated before [3]. In other words, the electrospray improves the performance of the condenser if there is a bottleneck in vapor delivery to the condensing wall. If the cooling power is excessive and there is a high gradient of vapor density toward the condensing surface, there is no room for improvement.

C. Experimental Data for Electrospray at Varied Ambient Humidity

For the direct investigation of water vapor nucleation on charged nucleus, we use the Phase Doppler Interferometry system (TSI FSA3500-2P). Four laser beams were aligned for the intercrossing at the axis of electrospray as shown in Fig. 6.

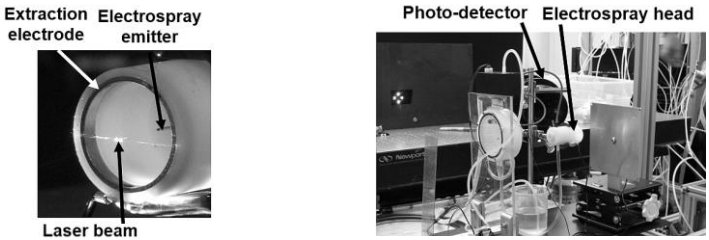

(a) (b)

Fig. 6. Phase Doppler interferometry of electrospray: (a) The electrospray head; (b) The total setup.

Due to the design of used electrospray head shown in Fig. 4(b), the measurements were possible only starting from the frontal edge of the head (15 mm from the emitter). Other limitations are related to the used equipment, which was able to detect droplets only with-

in size range from 1 μm to 1 mm. Fig. 5 presents the share of detected particles vs the measured axial velocity that clearly illustrates the deceleration of droplets (decreasing of terminal velocity) due to the elevated drag in air.

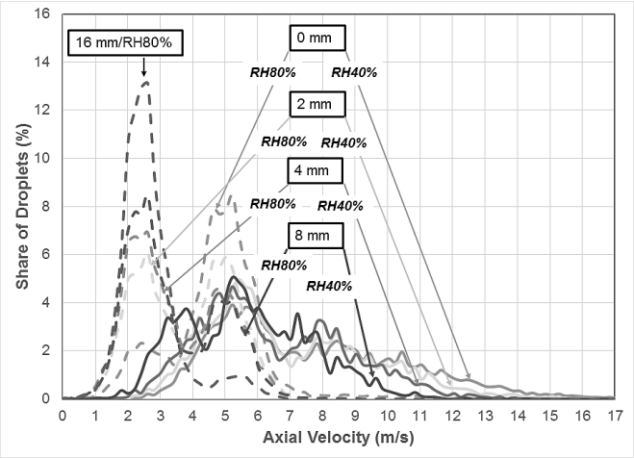

Fig. 5. Deceleration of particles due to the growth at varied distances from the electrospray head for normal humidity (RH40%), solid lines and elevated humidity (RH80%), dash-lines.

Fig. 6 illustrates how the change of air humidity affects the distribution of droplet sizes at varied distances along the spray axis. Due to the intensive background droplet content as a result of vapor condensation on ions of natural ionization, droplets smaller than 50 mm are excluded from the statistics.

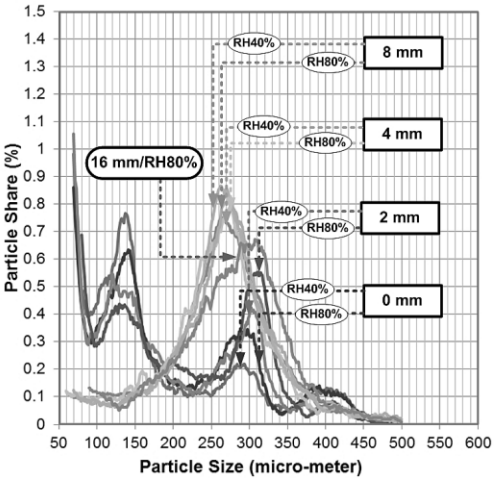

Fig. 6. Effect of air humidity on the distribution of droplets at varied distances along the spray axis.

In Fig. 6, all peaks in the range from 200 μm to 400 μm are either increased in magnitude or/and slightly shifted toward bigger particles when the humidity is increased. There

is no data for 16 mm distance at the normal humidity because the measurement provided statistically negligible data. Also, the share of small size (below 200 μm) particles is notably decreased at far distances (>4 mm) from the electrospray head. This should be attributed to the growth of small droplets while protracting from the emitter.

IV. Conclusion

The feasibility of evaluated concept for the electrostatic enhancement of water vapor harvesting from the air is experimentally proved. The five-fold improvement of the water collection rate with the improvised, non-optimized prototype is demonstrated.

V. Acknowledgment

This material is based upon work supported by the Small Business Innovative Research (SBIR) Program and the Engineering Research and Development Center (ERDC) – Construction Engineering Research Laboratory (CERL) under Contract W9132T-15-C-0011.

References

[1] M. Reznikov, "Dielectrophoretic Dehumidification of Gas Stream in Low and Moderate Electrical Fields," *Proc. ESA-IEEE Joint Meeting of Electrostatics, Little Rock, AR*, June 24 27, 2003, pp. 230-240.

[2] M. Reznikov, "Electrically Enhanced Condensation I: Effects of Corona Disch*arge," IEEE Trans. Industry Applications*, vol. 51, no. 2, 2015, pp. 1137-1145.

[3] M. Salazar K. Minakata, M. Reznikov, "Electrically Enhanced Condensation II: Effects of the Electrospray*," IEEE Trans. Industry Applications*, vol. 51, no. 2, 2015, pp. 1146-1152.

[4] A. E. K. Sundén, K. Støchkel, S. Panja, U. Kadhane, P. Hvelplund, S. B. Nielsen, H. Zettergren, B. Dynefors, and K. Hansen, "Heat capacities of freely evaporating charged water clusters," *J. Chem. Phys.*, vol. 130, 224308(7), 2009.

[5] F. Yu, "Modified Kelvin–Thomson equation considering ion-dipole interaction: Comparison with observed ion-clustering enthalpies and entropies," *J. Chem. Phys*., vol. 122, 084503, 2005.